

Calculation Method for the Bandgap of Antimonide Based Multicomponent Alloys

N. AN*, C.Z. LIU, C.B. FAN, X. DONG AND Q.L. SONG

Changchun Observatory/NAO, Chinese Academy of Sciences, Changchun 130117, China

(Received July 29, 2016)

As the most important material parameter of semiconductor, bandgap is necessary to be investigated to meet the design requirements of the high-performance optoelectronic devices. A new method of is proposed to calibrate the bandgap of antimonide based multi-component alloys with considering the effect of spin-orbit splitting off bands and the doublet degeneracy of valance band on the bandgaps of Sb-containing materials. A correction factor is introduced in the conventional calculation, and the spin-orbit splitting method is proposed. Besides, the $\text{In}_x\text{Ga}_{1-x}\text{As}_y\text{Sb}_{1-y}$ films with different compositions are grown on GaSb substrates by molecular beam epitaxy, and the corresponding bandgaps are obtained by photoluminescence to test the accuracy and reliability of this new method. An error rate analysis reveals that the α calculated by the spin-orbit splitting correction method is decreased to 2%, almost one order of magnitude smaller than the Moon method, which means that the new method can calculate the antimonide multicomponent more accurately with some applicability. This work can give a reasonable interpretation for the reported results and beneficial to tailor the antimonides properties and optoelectronic devices.

DOI: [10.12693/APhysPolA.133.118](https://doi.org/10.12693/APhysPolA.133.118)

PACS/topics: 81.05.Ea, 42.55.Px, 81.15.Hi

1. Introduction

The III-V semiconductor material system (GaIn)(AsSb) establishes a firm platform for optoelectronic devices operating near the mid-infrared spectral range (2–3 μm). The devices based on the antimonides have been intensively developed in recent years with the potential applications in a wide variety of areas such as material processing, secure free-space communication, infrared countermeasures, and atmospheric pollution monitoring [1–3].

The bandgap of multicomponent materials are the basement to research the structural design and fabrication of high-performance Sb-containing optoelectronic device. It can be obtained from the photon luminescence spectroscopy, infrared absorption spectroscopy, the cyclotron resonance experiments etc., which are difficult and complicated [4–6]. For the numerical techniques and analysis, the research on the materials bandgap developed slowly in the past decades and the correlative reports are very few. At the present, the Moon method proposed in 1974 is still the major way in the structure design and simulation, which has a low precision and cannot satisfy the modern optoelectronic apparatus requirements [7, 8].

In this paper, the band structure of antimonide based multicomponents materials are systematically investigated. The spin-orbit splitting correction method is presented in the calibration of the antimonide materials bandgap by considering the effect of spin-orbit splitting

off bands and degeneracy of valance band on the band structure. In order to confirm the validity and practicality of new method, the $\text{In}_x\text{Ga}_{1-x}\text{As}_y\text{Sb}_{1-y}$ films with different compositions are grown on GaSb substrates by molecular beam epitaxy (MBE), and the corresponding bandgaps are obtained by photoluminescence (PL).

2. Theoretical analysis

Antimonide based multicomponent alloys mainly refer to the Sb-containing binary, ternary and quaternary compounds, consisting of the III-group elements (Ga, In, Al, etc.) and V-group elements (As, Sb, etc.). Compared with the single-component semiconductor materials, the calibration of multicomponent alloys parameters is more complicated and difficult, which is usually derived with the binary or ternary compounds parameters. Taking $\text{In}_x\text{Ga}_{1-x}\text{As}_y\text{Sb}_{1-y}$ as an example, the schematic diagram of calibrating quaternary semiconductor material parameters are shown in Fig. 1.

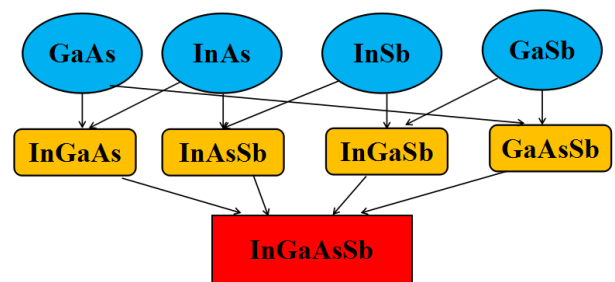


Fig. 1. Relationship between the parameters of binary, ternary, quaternary antimonides semiconductor compounds.

Nowadays, the Moon method is usually used to com-

*corresponding author; e-mail: anning4252@126.com

pute the bandgap of semiconductor materials. The main idea of the method is dividing the quaternary antimonide into four binary related materials. $\text{In}_x\text{Ga}_{1-x}\text{As}_y\text{Sb}_{1-y}$, for example, it is considered as an aggregation of InAs, GaSb, GaAs, and InSb. The bandgap of $\text{In}_x\text{Ga}_{1-x}\text{As}_y\text{Sb}_{1-y}$ is decided in the following formula:

$$E_g^{\text{In}_x\text{Ga}_{1-x}\text{As}_y\text{Sb}_{1-y}} = xyE_g^{\text{InAs}} + x(1-y)E_g^{\text{InSb}} \\ + (1-x)yE_g^{\text{GaAs}} + (1-x)(1-y)E_g^{\text{GaSb}} \\ - x(1-x)yC_\Gamma^{\text{InGaAs}} - x(1-x)(1-y)C_\Gamma^{\text{InGaSb}} \\ - xy(1-y)C_\Gamma^{\text{InAsSb}} - (1-x)y(1-y)C_\Gamma^{\text{GaAsSb}}. \quad (1)$$

Here, E_g is the bandgap of binary semiconductor materials, C_Γ is the bowing parameters of Γ bands in ternary compounds. The related concrete parameters are shown in Tables I and II.

TABLE I
Bandgap of III-V group binary compounds [9].

Binary material	E_g	Δ_0
InAs	0.359	0.38
InSb	0.17	0.81
GaAs	1.43	0.34
GaSb	0.72	0.82

TABLE II
Bowing parameters of III-V group ternary compounds bands [9].

Ternary material	Γ	X	L	Δ
InGaAs	0.6	1.4	0.72	0.2
InGaSb	0.42	0.33	0.38	0.1
GaAsSb	1.2	1.09	1.09	1.61
InAsSb	0.58	0.59	0.57	1.2

The structural diagram of InGaAsSb is indicated in Fig. 2. For InGaAsSb, the conduction band includes Γ band, X band, and L band, while the valence band has light hole band, heavy hole band, and splitting-off band. By definition, the bandgap is equal to the energy difference between the bottom of conduction band and the top of valence band. Both of the above two points is set in the valley of Γ band for InGaAsSb, so the bowing parameters that the Moon method used is the Γ band.

However, by comparing the material parameters in Table I, it can be identified that the bandgaps of most splitting off bands are greater than Γ bands, which means the effects of split off band on the bandgap cannot be ignored and the bowing parameters of splitting-off band should also be used in the bandgap calibration. Besides, because the tops of heavy hole band and light hole band are coincident at the highest point of valence band, the degeneracy of valence band should be another key element to the bandgap of antimonides.

In order to obtain the more precise bandgap of InGaAsSb in theory, a spin-orbit splitting correction factor t is introduced in the calibration for the unique band structure of $\text{In}_x\text{Ga}_{1-x}\text{As}_y\text{Sb}_{1-y}$:

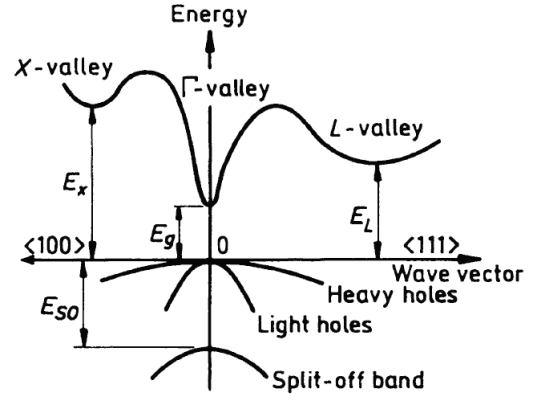


Fig. 2. Diagram of InGaAsSb band structure.

$$t = \frac{1}{2} \left[x(1-x)yC_\Delta^{\text{InGaAs}} + x(1-x)(1-y)C_\Delta^{\text{InGaSb}} \right. \\ \left. + xy(1-y)C_\Delta^{\text{InAsSb}} + (1-x)y(1-y)C_\Delta^{\text{GaAsSb}} \right]. \quad (2)$$

Here, x and y are the contents of different elements, and C_Δ are the bowing parameters of splitting-off band in ternary semiconductor compounds. Due to the doublet degeneracy of valence band, the $1/2$ coefficient is introduced in the spin-orbit splitting correction factor.

Hence, based on the Moon method, the spin-orbit splitting correction method is proposed as the following formula:

$$E_g^{\text{In}_x\text{Ga}_{1-x}\text{As}_y\text{Sb}_{1-y}} = xyE_g^{\text{InAs}} + x(1-y)E_g^{\text{InSb}} \\ + (1-x)yE_g^{\text{GaAs}} + (1-x)(1-y)E_g^{\text{GaSb}} \\ - x(1-x)yC_\Gamma^{\text{InGaAs}} - x(1-x)(1-y)C_\Gamma^{\text{InGaSb}} \\ - xy(1-y)C_\Gamma^{\text{InAsSb}} - (1-x)y(1-y)C_\Gamma^{\text{GaAsSb}} \\ + \frac{1}{3}(x(1-x)yC_\Delta^{\text{InGaAs}} - x(1-x)(1-y)C_\Delta^{\text{InGaSb}} \\ - xy(1-y)C_\Delta^{\text{InAsSb}} - (1-x)y(1-y)C_\Delta^{\text{GaAsSb}}). \quad (3)$$

3. Results and discussion

In order to validate the theoretical results, the $\text{In}_{0.25}\text{Ga}_{0.75}\text{As}_{0.08}\text{Sb}_{0.92}$ and $\text{In}_{0.2}\text{Ga}_{0.8}\text{As}_{0.02}\text{Sb}_{0.98}$ thin films are grown on GaSb substrates by DCA P600 MBE SYSTEM, and the experimental values of antimonide bandgaps are obtained by photoluminescence. Figure 3 shows the PL spectra of $\text{In}_{0.25}\text{Ga}_{0.75}\text{As}_{0.08}\text{Sb}_{0.92}$ and $\text{In}_{0.2}\text{Ga}_{0.8}\text{As}_{0.02}\text{Sb}_{0.98}$ thin films at room temperature.

According to the analysis and results above, the theoretical results of $\text{In}_{0.25}\text{Ga}_{0.75}\text{As}_{0.08}\text{Sb}_{0.92}$ and $\text{In}_{0.2}\text{Ga}_{0.8}\text{As}_{0.02}\text{Sb}_{0.98}$ calibrated by the Moon method and the spin-orbit splitting method are indicated in Table III. Compared with the experimental values, the relative error α of calibration results using different methods is obtained by the following formula:

$$\alpha = \frac{|\text{theoretical value} - \text{experimental value}|}{\text{experimental value}} \times 100\%.$$

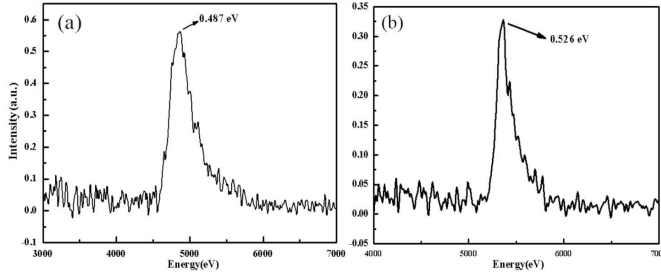


Fig. 3. PL spectra of InGaAsSb/GaSb at room temperature: (a) $\text{In}_{0.25}\text{Ga}_{0.75}\text{As}_{0.08}\text{Sb}_{0.92}$, (b) $\text{In}_{0.2}\text{Ga}_{0.8}\text{As}_{0.02}\text{Sb}_{0.98}$.

(4)

From Table III, it can be seen that the bandgap calibrated by the spin-orbit splitting method is closer to the experimental values, the relative error α is reduced by almost 7 times, which suggests that the new method is superior to the common Moon method for antimonide based multicomponents bandgap.

TABLE III

Error rates [%] of two calculation methods for $\text{In}_x\text{Ga}_{1-x}\text{As}_y\text{Sb}_{1-y}$ bandgaps [eV].

Compound	Exp.	Moon	S.-o.	α_M	α_{so}
$\text{In}_{0.25}\text{Ga}_{0.75}\text{As}_{0.08}\text{Sb}_{0.92}$	0.487	0.449	0.496	7.8	1.8
$\text{In}_{0.2}\text{Ga}_{0.8}\text{As}_{0.02}\text{Sb}_{0.98}$	0.526	0.493	0.532	6.8	0.9

TABLE IV

Experimental values and calculation methods error rates [%] of $\text{In}_x\text{Ga}_{1-x}\text{As}_y\text{Sb}_{1-y}$ bandgaps [eV].

	x	y	Exp.	Moon	S.-o.	α_M	α_{so}
1[10]	0.06	0.05	0.649	0.630	0.650	2.92	0.15
2[12]	0.207	0.100	0.528	0.483	0.523	8.5	0.94
3[11]	0.15	0.140	0.569	0.514	0.562	9.67	1.23
4[13]	0.18	0.170	0.539	0.481	0.538	10.76	0.19
5[14]	0.18	0.14	0.549	0.489	0.539	10.93	1.82
6[12]	0.241	0.119	0.506	0.449	0.498	11.26	1.58

To go a step further and evaluate the applicability of spin-orbit splitting method, the bandgaps of InGaAsSb with other contents reported before are also computed by the above two methods, shown in Table IV. It concludes that the new method is more applicable for the calibrating of the antimonide based multicomponent, and the results are approximate to the experimental values, the relative α decreases by an order of magnitude, approximately below 2%.

4. Conclusion

The methods for computing the bandgap of antimonide based multicomponent alloys are investigated based on the analysis of the antimonides band structure. Considering the effects of spin-orbit splitting off bands and the doublet degeneracy of valence band on

the bandgap of Sb-containing compounds, a correction factor is introduced in the calibration, and the spin-orbit splitting method is proposed. In order to validate the accuracy and reliability of new method, the $\text{In}_{0.25}\text{Ga}_{0.75}\text{As}_{0.08}\text{Sb}_{0.92}$ and $\text{In}_{0.2}\text{Ga}_{0.8}\text{As}_{0.02}\text{Sb}_{0.98}$ thin films are fabricated on GaSb substrates by molecular beam epitaxy and the experimental values are obtained by photoluminescence. The results show that the theoretical values computed by the spin-orbit splitting method is closer to the experimental values, the corresponding error α is only 1.8% and 0.9%, far less than the conventional Moon method. When InGaAsSb has other contents, the new method are still more applicable, the α are decreased to 2%, almost one order of magnitude smaller than the results of the Moon method, which means the spin-orbit splitting method can be instead of the Moon method to calibrate the bandgap of antimonide based multicomponent alloys precisely. This work can give a reasonable interpretation for the reported results and beneficial to tailor the antimonide property and photonics devices.

References

- [1] R. Ahmed, S.J. Hashemifar, H.H. Akbarzadeh, *Commun. Theor. Phys.* **3**, 52 (2009).
- [2] H.W. Xu, Y.Q. Ning, Y.G. Zeng, X. Zhang, L. Qin, *Opt. Precision Eng.* **3**, 21 (2013).
- [3] D. Liu, Y.Q. Ning, J.L. Zhang, X. Zhang, L.J. Wang, *Opt. Precision Eng.* **10**, 20 (2012).
- [4] P.J. Collings, *Am. J. Phys.* **3**, 48 (1980).
- [5] K. Busch, S. John, *Phys. Rev. E* **3**, 58 (1998).
- [6] S. Adachi, *J. Appl. Phys.* **10**, 61 (1987).
- [7] R.L. Moon, G.A. Antypas, L.W. James, *J. Electron. Mater.* **3**, 3 (1974).
- [8] N. An, Z.G. Zhan, B.T. He, P. Lu, X. Fang, Z.P. Wei, G.J. Liu, *High Power Laser Part. Beams* **26**, 11 (2014).
- [9] R.J. Kumar, R.J. Gutmann, J. Borrego, P.S. Dutta, C.A. Wang, R.U. Martinelli, G. Nichols, *J. Electron. Mater.* **33**, 2 (2004).
- [10] K. Shim, H. Rabitz, P. Dutta, *J. Appl. Phys.* **12**, 88 (2000).
- [11] J.C. DeWinter, M.A. Pollack, A.K.J.L. Zyskind, *J. Electron. Mater.* **6**, 14 (1985).
- [12] W.G. Bi, A.Z. Li, Y.L. Zheng, J.X. Wang, C.C. Li, *J. Infrared Millim. Waves* **5**, 11 (1992).
- [13] J.L. Zyskind, C.A. Burrus, C. Caneau, A.G. Dentai, M.A. Pollack, A.K. Srivastava, J.E. Bowers, J.C. DeWinter, *Proc. SPIE* **722**, (1987).
- [14] P.S. Dutta, A.G. Ostrogorsky, *J. Cryst. Growth* **198-199**, 384 (1999).